AIAA JOURNAL
Vol. 41, No. 7, July 2003

Beamforming Algorithm for Distributed Source Localization and Its Application to Jet Noise

Saligrama R. Venkatesh*
Boston University, Boston, Massachusetts 02215
and
David R. Polak† and Satish Narayanan‡
United Technologies Research Center, East Hartford, Connecticut 06108

A new algorithm for estimating noncompact, distributed sources by means of phased array microphone measurements is presented and experimentally implemented to determine the noise source distribution in a subscale jet flow. Conventional beamforming techniques, developed for spatially well-separated point sources, can lead to significant errors when applied to reconstruct continuous source distributions such as jet noise. A new beamforming approach is developed for estimating such continuous source distributions. The objective is to recover the average source strength over a small region around each focus position as opposed to seeking the exact source strength at each spatial location as in conventional approaches. This strategy overcomes the drawbacks of conventional methods and yields a beamformer with uniform spatial resolution and accuracy over a large frequency range. The measurement technique is applied to the localization of broadband noise sources in a high-subsonic, heated, turbulent jet flow and shows good comparisons with prior measurements using other techniques.

Nomenclature

c	=	ambient sound speed, m/s
D_{jet}	=	nozzle diameter, m
f	=	frequency, Hz
$G(f, x)$	=	nondimensional steering matrix
$H(f, x)$	=	source to receiver propagation matrix, m^{-1}
M_{jet}	=	jet exit Mach number
n	=	number of microphones
p_{ref}	=	reference acoustic pressure, Pa
$r_j(x)$	=	propagation distance from source at x to jth microphone, m
r_0	=	reference distance, m
Sr	=	Strouhal number, $f D_{\text{jet}}/U_{\text{jet}}$
$s(t, x)$	=	source strength, Pa
T_{jet}	=	jet exit temperature, °C
t	=	time, s
U_{jet}	=	jet exit centerline velocity, m/s
$W(f, x)$	=	beamformer weights for frequency f and location x, m
$w(f, x)$	=	nondimensional beamformer weights for frequency f and location x
$w_\delta(x)$	=	Dirac delta function
x	=	spatial location, m
x_0	=	focal point location, m
$\boldsymbol{Y}(\cdot)$	=	column vector of microphone measurements, Pa
$y_j(t)$	=	sound pressure measured at jth microphone, Pa
$\Gamma_s(f, x)$	=	source strength propagated to radius r_0, Pa^2/Hz
δ	=	localization parameter that defines the source region, m
$\zeta_s(f, x, \mu)$	=	source cross spectral density between positions x and $x + \mu$, at frequency f, Pa^2/Hz
ρ	=	accuracy parameter in optimization problem
$\Phi_s(f, x)$	=	source strength per unit length at frequency f and position x, Pa^2m/Hz
$\Phi_Y(f)$	=	cross spectral density matrix of microphone measurements, Pa^2/Hz
$\Psi_s(f, x)$	=	$\hat{\Phi}_s(f, x)$ from the previous estimate in a recursive processing scheme, Pa^2m/Hz
Ω	=	spatial extent of source, m
$*$	=	conjugate transpose
$\wedge$	=	estimated quantity
-	=	spatially averaged quantity

Received 22 March 2002; revision received 6 February 2003; accepted for publication 22 February 2003.

*Assistant Professor, Department of Electrical and Computer Engineering.
†Research Engineer, Systems Department. Member AIAA.
‡Associate Fellow, Systems Department. Member AIAA.

I. Introduction

THE need to reduce aircraft exhaust noise emissions has led to numerous studies aimed at understanding the underlying noise sources and applications of source localization techniques to jet noise.[1–10] Computational aeroacoustics methods, capable of resolving flowfield details simultaneously with noise radiation,[11] are yet unable to simulate acoustics reliably at realistic flow conditions, for example, complex geometry and high Reynolds numbers. On the other hand, state-of-the-art experimental techniques (also typically limited to low Reynolds numbers, Mach numbers, and temperature) are limited in the spatiotemporal resolution needed to resolve the relevant flowfield details. We utilize a newly developed source localization technique to enable a more detailed exploration of jet noise generation at realistic Mach and Reynolds numbers. Accurate estimates of the spatial distribution of the sources can provide insights into the noise-generation mechanisms and their connection with the complex turbulent flowfield, validate computational aeroacoustic models, and guide the design of noise-reduction technologies.[10]

In particular, microphone phased array processing techniques, capable of revealing the spatial distribution of noise sources, are becoming more widely used. The principal idea for such techniques is to sum the measurements coherently at different microphones to enhance the signal emanating from a focal position while minimizing the contribution from out-of-focus locations.[12] Phased array design involves two steps: The first step is the choice of geometric locations for the microphones, and the second step, which is the focus of this paper, is to specify a rule, referred to as beamforming, for appropriate summation of the microphone measurements to reconstruct the spatial distribution of noise sources.

For the simplest delay-and-sum beamformer, the outputs of time-delayed sensor measurements are summed, with the delays as a function of focus position and sensor location, to estimate the source distribution.[12] When a source is at the focus position, the signals add coherently to produce an enhanced signal, whereas for out-of-focus positions, the signals add incoherently. The performance of this simple beamformer can be improved by weighting or shading the microphone signals before summation.

Although such conventional beamforming techniques work well in locating a multiple set of isolated point sources, they can perform poorly when reconstructing continuously distributed noise sources such as jet noise. Indeed, for applications such as airframe noise,[13–15] aircraft flyover noise,[16–18] and vehicle passby noise,[19,20] where conventional techniques have successfully yielded important information about the dominant acoustic sources, either a single source was found to dominate at a particular frequency or several sources dominated but were well separated in space. Phased array measurements of jet noise have also been conducted[9] where the problem is to estimate a continuous source distribution rather than simply locating dominant sources. This is a significantly more challenging beamforming problem, where contributions from out-of-focus sources can lead to unacceptable estimation errors. This difficulty has been largely overlooked in the literature, and this paper presents a new beamforming approach for estimating distributed noise sources. The main idea is to recover the average source strength over a small region around each focus position as opposed to seeking the exact source strength at each spatial location as in conventional approaches. This overcomes the drawbacks of conventional methods of estimating continuous distributions and yields a beamformer with uniform spatial resolution and accuracy over a large frequency range.

The organization of the paper is as follows. First, the main problems encountered in beamforming a distribution of sources are outlined. Next, a beamforming algorithm that overcomes these problems is presented. The tradeoff between spatial resolution and accuracy of the estimate is described. Experiments to validate the processing algorithm are then discussed, where the performance of the technique developed here is compared to that from the minimum variance beamformer. Finally, some results from the application of the new array processing approach to jet noise source localization using measurements from a linear phased array are presented and compared with prior studies.

II. Phased Array Processing

In this section, we outline a new scheme for phased array processing of distributed sources. We will present the setup, outline the shortcomings of current approaches, and finally illustrate the new approach. The main ideas in the new formulation are 1) definition of spatial resolution as a localized spatial average of the source distribution (as opposed to the traditional definition of spatial resolvability of two discrete sources) and 2) ability to tune spatial resolution for achieving desired accuracy.

A. Problem Setup

The setup consists of sound incident on an n-microphone array from a broadband, radially compact, axially noncompact, axisymmetric distribution of monopoles along the jet centerline of length Ω. The instantaneous source strength $s(t, x)$ radiated from a source at location x at time t is assumed to be a stationary random field. Based on a spherical wave propagation model at ambient sonic speed c, we can relate the jth instantaneous microphone measurement $y_j(t)$ to the source strength $s(t, x)$:

$$\boldsymbol{y}_j(t) = \int_\Omega \frac{1}{r_j(x)} s\left[t - \frac{r_j(x)}{c}\right] \mathrm{d}x \tag{1}$$

where $r_j(x)$ is the propagation distance from the source at x to the jth microphone. We collect all of the measurements at each time instant into a matrix $\boldsymbol{Y}(t)$ [with $\boldsymbol{y}_j(t)$ as column vectors] and compute the cross spectral density (CSD) matrix . The CSD matrix Φ_Y is a linear function of the source CSD, ζ_s:

$$\Phi_Y(f) = \iint_\Omega H(f, x)\zeta_s(f, x, \mu)H^*(f, x + \mu)\,\mathrm{d}x\,\mathrm{d}\mu \tag{2}$$

where $\zeta_s(f, x, \mu)$ is the CSD of the source between points x and $x + \mu$ and $H(f, x)$ is

$$H(f, x) = \begin{bmatrix} [1/r_1(x)]\exp[-i2\pi f r_1(x)]/c \\ \vdots \\ [1/r_n(x)]\exp[-i2\pi f r_n(x)]/c \end{bmatrix} \tag{3}$$

with H^* as its conjugate transpose. When the source is assumed to be axially uncorrelated, Eq. (2) simplifies to

$$\Phi_Y(f) = \int_\Omega H(f, x)\Phi_s(f, x)H^*(f, x)\,\mathrm{d}x \tag{4}$$

where Φ_s is the source strength per unit length along the jet centerline. The objective is to reconstruct the source distribution Φ_s from the measured CSD Φ_Y.

Φ_Y has n rows and n columns, whereas the source distribution is a function of a continuous variable x. Therefore, the problem involves solving a linear system of a finite number of equations with infinitely many unknowns, leading to an ill-posed nature. Such ill-posed problems have been studied in the general area of inverse problems.[21] An exact reconstruction of the power spectral density (PSD) of the source distribution is impossible, and in general, one seeks approximate solutions. Conventional phased array processing in aeroacoustics has used well-known radar/sonar signal processing techniques. These techniques have been developed for isolation and detection of a finite number of point sources, and it is our contention that such techniques are inadequate for the distributed source estimation problem. In the next section, we briefly describe array geometry issues and subsequently develop a beamforming approach for distributed source estimation.

B. Array Geometry

The simplest array geometry consists of uniformly spaced microphones arranged in a straight line parallel to the array axis. It is well known that the maximum frequency resolvable by a uniform array without spatial aliasing is limited by the spacing between the microphones. On the other hand, spatial resolution is proportional to the ratio of the wavelength to the aperture of the array. Good spatial resolution at both low and high frequencies implies that a large aperture is required with small spacing, resulting in a prohibitively large number of microphones. Sparse arrays, with nonuniform microphone spacing, help to overcome this difficulty by exploiting the fact that higher frequencies require a relatively smaller aperture to achieve the same spatial resolution. The comparison of nonuniform arrays to uniform arrays has been extensively studied in the literature.[22] Random microphone spacings are a commonly used form of nonuniform arrays. Another arrangement is the orthogonal restricted difference basis (ORDB)[22] array, used in the present study. This geometry consists of two nested uniform arrays, one with small interelement spacing and the other with coarse spacing. Although this may appear to offer little improvement over a uniform array, it in fact produces a diverse set of phase relationships when considering microphone pairings between the fine array and a given microphone from the coarse array. An illustration of the advantages of ORDB arrays is provided in Fig. 1, which is a comparison of the ORDB array performance to an array having a random distribution of microphone spacings. Minimum variance beamforming, a technique described in the following section, was used to compute the array response for both array geometries. The ORDB array achieves excellent beamwidth (spatial resolution) and sidelobe (rejection of off-axis directions) characteristics for both low and high

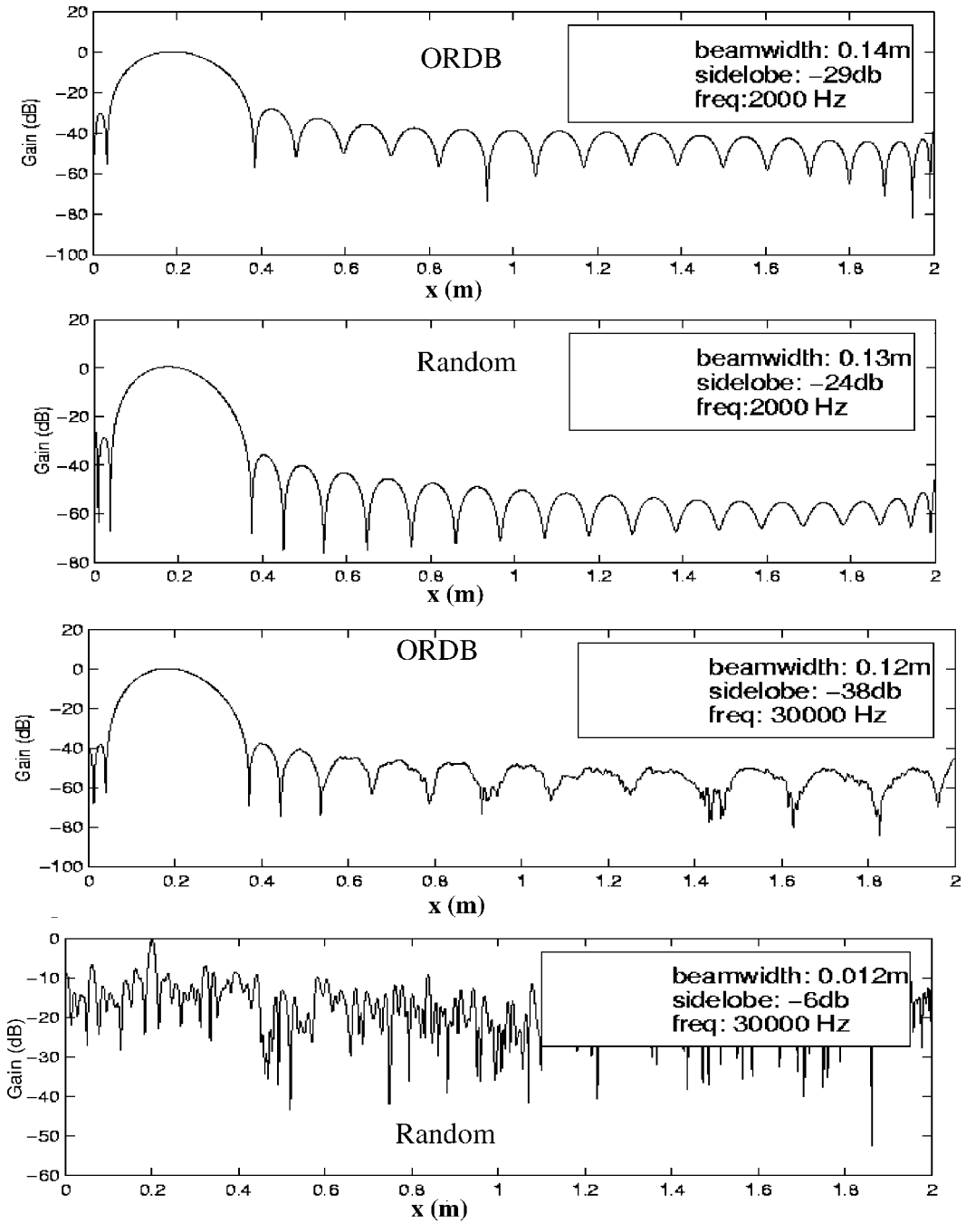

Fig. 1 Comparison of the array response for low- and high-frequency sources with different geometries.

frequencies. The simulations justify our use of ORDB arrays for broadband point source estimation. Nevertheless, array design is only one aspect of the problem, and once the microphone locations are chosen, there remains the beamforming problem, where a stable, accurate processing algorithm is sought. In the following, we briefly survey these techniques and discuss their drawbacks for distributed source localization.

C. Conventional Approaches

In the delay and sum technique, microphone measurements $y_j(t)$ are sequentially delayed and summed to form an estimate of the source strength. For processing in the frequency domain, the source region on the right-hand side of Eq. (4) is first discretized into a finite collection of lumped sources and then inverted:

$$\hat{\Gamma}_s(f,x) = (1/n^2)G^*(f,x)\Phi_Y(f)G(f,x) \tag{5}$$

where $G(f,x)$ is the nondimensional steering matrix

$$G(f,x) = \begin{bmatrix} [r_1(x)/r_0]\exp[-i2\pi f r_1(x)]/c \\ \vdots \\ [r_n(x)/r_0]\exp[-i2\pi f r_n(x)]/c \end{bmatrix} \tag{6}$$

and r_0 is a reference distance. Equation (6) is a simple but stable beamforming algorithm, which has been used successfully in a number of applications where a single source was dominant[14,15] and even for moving sources.[16,17,20] One drawback of Eq. (6) is the lack of independent control over the beamformer's spatial resolution and sidelobe levels. Another drawback is that the only way to improve the array performance is to add microphones.

Weighting, or shading, can improve the array performance. The weights for all of the microphones are collected in a vector $\boldsymbol{w}(f,x)$, and the estimate for the source strength at location x and

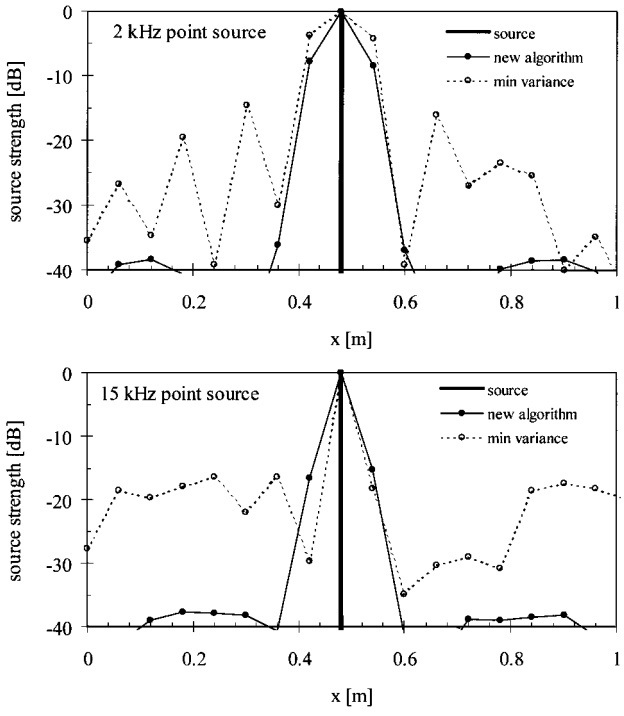

Fig. 2 Comparison of simulated minimum variance and new beamforming schemes for a point source at 2 and 15 kHz.

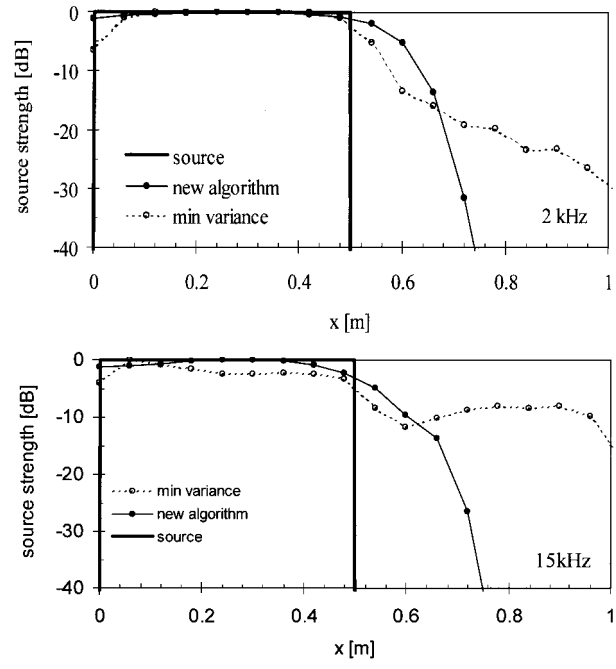

Fig. 3 Comparison of simulated minimum variance and new beamforming schemes for a distributed source at 2 and 15 kHz.

frequency f is given by

$$\hat{\Gamma}_s(f,x) = (1/n^2)G^*(f,x)\boldsymbol{w}(f,x)\Phi_Y(f)w^*(f,x)G(f,x) \quad (7)$$

In minimum variance beamforming, the objective is to minimize the total energy while passing signals unattenuated from the desired focal point. The resulting weights are given by

$$\boldsymbol{w}(f,x) = \frac{\Phi_Y^{-1}(f,x)}{G^*(f,x)\Phi_Y^{-1}(f)G(f,x)} \quad (8)$$

Often, $\Phi_Y(f)$ is singular, so that some form of stabilization technique is required. Minimum variance beamforming has been used by several researchers.[9] Others have applied different weighting schemes.[23] The minimum variance approach effectively estimates point sources over a broad range of frequencies. This is seen from numerical simulations such as that in Fig. 2, where a broadband point source of unit magnitude at a location 1.63 m away from and 0.5 m along the array axis is accurately located and estimated at both low and high frequencies. For a single point source, when the focal position coincides with the source location, there are no other sources to corrupt the estimated source strength. However, when the focus position is not the same as the source location, erroneous reconstructed source strength, or sidelobe level, is caused by the processing scheme's inability to completely null the source.

Such point source estimation is not sufficient for distributed sources. This is shown in Fig. 3 through numerical simulations for a 2- and 15-kHz uniformly distributed source at a distance of 1.63 m from the array. The source has a uniform strength over a length of 0.5 m along the array axis. Evidently, the minimum variance technique exhibits significant errors at 15 kHz.

The reason for the inaccuracy is the following. Unlike a single point source, the focus position can never completely coincide with the source location. This implies that there will always be nonzero contributions to the source strength estimate at a particular focal point due to contributions from sources at other locations. Although the same situation occurs in the context of a finite number of discrete sources, it turns out that as long as the number of sources is smaller than the number of microphones it is always possible to null their contributions.[22] Therefore, this problem of inaccurate estimates is specific to distributed sources. The problem of spurious sources as in Fig. 3 occurs because the sidelobe level is no longer a meaningful measure of the error. Rather, the integral of the aggregate source strength weighted by the sidelobe levels determines the error.

The minimum variance technique has difficulty estimating distributed sources because of two fundamental limitations. First, it fails to account for the fact that the array is unable to discriminate among sources in the neighborhood of the focus position. This is aggravated by the fact that sources within a small region are likely to be correlated. Thus, at the very least, the contribution from sources in the neighborhood of the focus position cannot be nulled. Therefore, the most that one can hope for is to find the average source strength in the neighborhood of the focus position. The second limitation of the minimum variance approach is that attempts to suppress all of the sources uniformly invariably leads to increased sidelobe levels. The large sidelobes shown in Fig. 3 at 15 kHz are a result of these limitations. In the next section, we describe a new beamforming approach that overcomes these shortcomings. A preview of the results has been illustrated in Figs. 2 and 3. It is seen that the new approach provides significantly better estimates for point as well as distributed sources for a broad range of frequencies.

D. New Beamformer: Localized Spatial Average

The new approach overcomes the difficulty with distributed sources by relaxing the objective of estimating the PSD $\Phi_s(f,x)$ in a pointwise fashion. Instead our objective is to estimate the average sound power radiated from a source interval δ:

$$\bar{\Phi}_s(f,x_0) = \frac{1}{\delta}\int_{x_0-\delta/2}^{x_0+\delta/2} \Phi_s(f,x)\,dx \quad (9)$$

The resulting PSD is a local average over a finite region of space, which is more appropriate for distributed sources. Furthermore, unlike minimum variance beamforming, the explicit inclusion of δ in the beamforming equations enables independent control over the spatial resolution and sidelobe levels.

We now describe how this relaxed objective of estimating the spatially averaged PSD overcomes the problems discussed in the preceding section. The localization or resolution parameter δ overcomes the fundamental limitation of the array to discriminate sources within a small neighborhood by incorporating the entire neighborhood of each location as part of the estimation objective. Moreover, larger δ implies smaller source regions outside the focal region. This implies that the beamformer will need to suppress less

of the undesirable signals. Thus, there is a tradeoff between accuracy and resolution explicitly built into the objective.

With these comments we can state the objective precisely: Determine the smallest resolution δ that still guarantees a desired level of accuracy. We now formalize this objective as a beamforming optimization problem.

The problem is to compute the beamformer weights that satisfy the localization and accuracy objectives. Once beamformer weights are obtained, the spatially averaged PSD is computed as in Eq. (7) except for a scaling by δ. Therefore, we are left with the problem of obtaining the beamformer weights. To capture the localization or resolution objective at a location x_0, we seek weights that satisfy

$$|W(f, x_0)H(f, x)| \approx 1, \qquad \forall x \in [x_0 - \delta/2, x_0 + \delta/2] \tag{10}$$

Note that the weights $W(f, x)$ have the dimension of length. To minimize contributions from sources outside the focal region around the location x_0, the weights are chosen such that the beamformed energy from the desired focal region is significantly larger than that received from outside the focal region. This can be accomplished by choosing beamformer weights that satisfy the following:

$$\int_{x \notin [x_0 - \delta/2,\, x_0 + \delta/2]} [W(f, x_0)H(f, x)]^2 \, dx \leq \rho \int_{x_0 - \delta/2}^{x_0 + \delta/2} [W(f, x_0)H(f, x)]^2 \, dx \tag{11}$$

The left-hand side of the equation is the beamformed energy contribution from outside the focal region, whereas the right-hand side is a scaling (with scaling parameter ρ) of the energy contribution from within the desired focal region. Thus, the ratio of outside energy contribution to the actual is measured by the parameter ρ. If a beamformer satisfying Eqs. (10) and (11) exists, it follows that a locally averaged PSD is given by

$$\hat{\bar{\Phi}}_s(f, x_0) = (1/\delta)W(f, x_0)\Phi_Y(f)W^*(f, x_0) \tag{12}$$

and the beamformer achieves the following accuracy:

$$|\bar{\Phi}_s(f, x_0) - \hat{\bar{\Phi}}_s(f, x_0)| \leq \frac{\rho}{\delta} \int_{\Omega} \Phi_s(f, x) w_\delta(x - x_0) \, dx \tag{13}$$

where w_δ is the Dirac delta function. The proof of this claim follows from rewriting the beamformed estimate and is provided in the Appendix. Equation (13) illustrates that the smaller the accuracy parameter ρ and the larger the localization parameter δ are the higher the accuracy of the estimated source strength. Note that the expression in Eq. (12) does not appear to be similar to Eq. (7). This difference can be mathematically explained by suitably redefining the beamformer weights $w(f, x)$ in Eq. (7) by absorbing the scaling factor n and the steering matrix G^*. More important, the size of the source region as the scaling factor in the PSD estimate makes explicit the objective of estimating the average PSD for a continuous distribution.

The optimization problem is to find a set of beamforming weights that result in the smallest localization for a satisfactory accuracy. Numerical simulations for the new beamforming technique have been compared with minimum variance beamforming at both low (2-kHz) and high (15-kHz) frequencies for point as well as distributed sources in Figs. 2 and 3. It is seen that the new technique exhibits significant improvements in both accuracy and localization. Minimum variance beamforming performs particularly poorly for high-frequency distributed sources. The improvements with the new beamformer are discussed next.

1. Tradeoffs

The two parameters δ and ρ can be tuned to obtain satisfactory localization with guaranteed levels of accuracy. Larger δ implies larger focal regions, which in turns means a smaller source region whose radiation needs to be suppressed in the PSD estimate. Generally, this leads to higher accuracy. Simulations (noise free) using the new beamforming technique are illustrated as a plot of resolution (in jet diameters D_{jet}) vs accuracy (sidelobe rejection) at 20 kHz in Fig. 4; the jet diameter used $D_{\text{jet}} \approx 0.083$ m. For $\frac{1}{8}D_{\text{jet}}$ resolution, the sidelobe rejection is 7 dB, whereas for $3D_{\text{jet}}$ the accuracy improves to -21 dB.

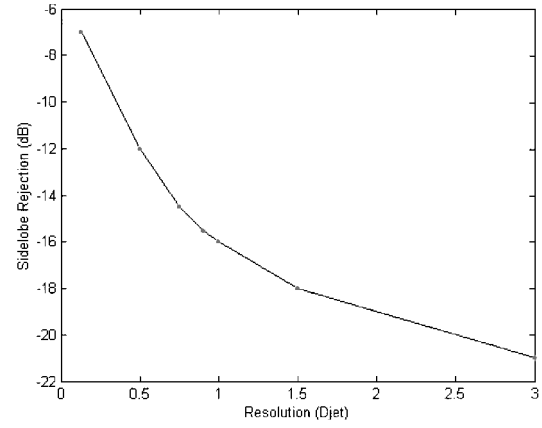

Fig. 4 Simulated tradeoff between spatial resolution and sidelobe rejection at 20 kHz with new beamforming algorithm.

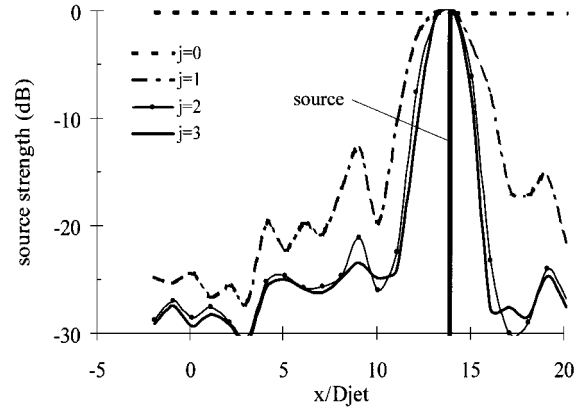

Fig. 5 Demonstration of new recursive processing algorithm for a 25-kHz point source.

2. Recursive Improvement in Accuracy

We have presented error bounds for the beamformer in Eq. (13). The beamformed estimate can be improved upon by using the PSD estimates found from solving Eq. (12). To do this, we solve a modified beamforming problem. To see this, let

$$\hat{\Psi}_s(f, x) = (1/\delta)W(f, x)\Phi_Y(f)W^*(f, x) \tag{14}$$

We know from Eq. (13) that this estimate closely approximates the spatially averaged PSD. One can make use of this information to improve the accuracy by modifying Eq. (11) as follows:

$$\int_{x \notin [x_0 - \delta/2, x_0 + \delta/2]} [W(f, x_0)H(f, x)]^2 \hat{\Psi}_s(f, x) \, dx \leq \rho \int_{x_0 - \delta/2}^{x_0 + \delta/2} [W(f, x_0)H(f, x)]^2 \hat{\Psi}_s(f, x) \, dx \tag{15}$$

This modification improves the accuracy of the beamformed estimates and can be performed recursively. The improvement occurs because smaller values of ρ will still satisfy the inequality. When there is a strong source at x_0, the right-hand side of Eq. (15) is increased. When this is not the case, weights can be chosen to minimize the left-hand side of Eq. (15) more easily. The algorithm is demonstrated in Fig. 5 for a 25-kHz point source located at $x/D_{\text{jet}} = 14$. Figure 5 was obtained not from a simulation but from actual data acquired in an anechoic facility and processed with the new algorithm,

where the beamformer output was converted to a source strength in decibels,

$$\hat{\Gamma}_s(f,x) = 10 \times \log_{10}\left[\frac{\delta \int_{f_1}^{f_2} \hat{\hat{\Phi}}_s(f,x)\,\mathrm{d}f}{p_{\mathrm{ref}}^2 r_0^2}\right] \qquad (16)$$

with $r_0 = 1$m. When a uniform distribution is assumed, the first pass through the algorithm locates the source with a fairly broad beamwidth and a sidelobe of −12 dB. Successive recursions reduce the beamwidth and increase the sidelobe rejection to −23 dB. The process converges after two or three recursions. By picking δ such that $\rho \ll 1$, we ensure that the PSD has high accuracy for the chosen spatial resolution.

3. Uniform Localization Across Frequency and Space

One of the main advantages of the algorithm is that one can obtain spectral density estimates across frequency and space with similar accuracy and resolution. This can be accomplished by picking a common resolution parameter δ and a satisfactory accuracy parameter ρ. The new beamforming algorithm achieves a nearly uniform sidelobe rejection with a fixed beamwidth (demonstrated in the following section). With conventional beamforming, as frequency increases the beamwidth decreases, implying that spatial resolution improves at higher frequencies. However, this is followed by a significant degradation in accuracy, resulting in poor performance of conventional techniques for high-frequency distributed sources. These aspects will be further addressed in a later section.

We finally make a brief comment on the tractability of the new beamforming problem. The problem presented in Eqs. (10) and (11) belongs to the general class of problems consisting of a quadratic cost function with quadratic constraints. For a single quadratic constraint, the problem can be readily solved with convex optimization techniques.[24]

E. Array Hardware and Validation

Figure 6 shows a schematic of the array mounted in the United Technologies Research Center (UTRC) Acoustic Research Tunnel[25,26] (ART) with the jet model. The array was parallel to the jet aerodynamic centerline (aligned to within 1 deg) at a distance of 1.65 m $\cong 20D_{\mathrm{jet}}$. The total array aperture was 2.70 m $\cong 32.6D_{\mathrm{jet}}$, composed of 36 6.35-mm-diam condenser microphones. The microphone spacing was based on the ORDB[22] scheme, with the first 18 microphones separated by 0.007 m and the last 18 microphones separated by 0.143 m. The actual microphone interelement spacing was measured with a micrometer with an error of less than 0.5 mm. Acoustic foam treated all exposed portions of the array support structure.

Each data channel was bandpass filtered between 0.5 and 40 kHz and simultaneously acquired at 100 kHz with 16-bit resolution. The source distributions were produced using 2.5 s of data, which were

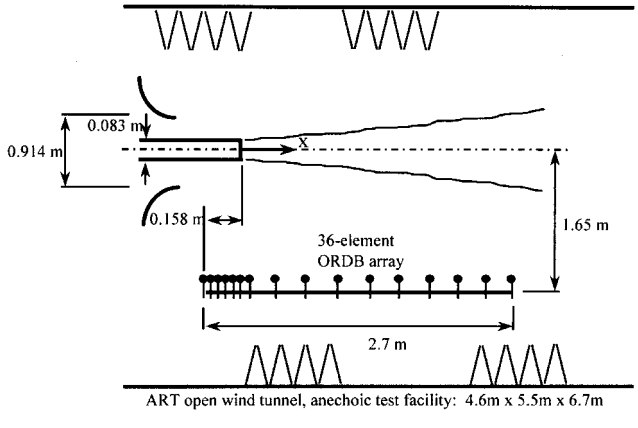

Fig. 6 Schematic of linear phased array and model-scale jet nozzle (not to scale) installed in anechoic facility.

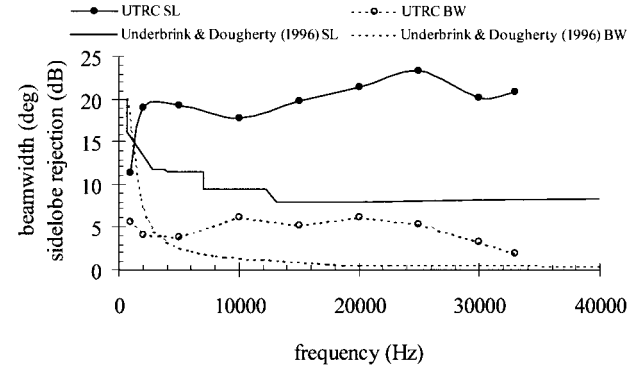

Fig. 7 Actual UTRC phased array performance compared with simulated[27] conventional array performance.

sufficient because the distributions statistically converged to better than 0.5 dB at all frequencies after 2.0 s of data. The amplitude response of the data acquisition system was calibrated by piston phone at 1 kHz. Because typical pretest and posttest results differed by less than 0.2 dB, the mean of the pre- and posttest amplitude corrections were applied to the raw data. Also, the phase response of the data acquisition system was measured by injecting broadband electrical noise into the microphone preamplifiers simultaneously. The maximum phase difference of any two channels at any frequency in the range 1–33 kHz was found to be less than 5 deg. Phase corrections were not applied to the raw data.

The array has been validated with a point source and a distributed broadband source. The point source was created with a 5-mm-diam air jet, whereas the distributed source was created with 16 air jets of 1.8 mm diameter evenly spaced along a 0.41-m tube. The sources were oriented so that the jet axes were perpendicular to the array, to create a point monopole source and a distributed (along array axis) source. The point and distributed air jet sources produced broadband noise in the range 1–35 kHz.

The point source was used to measure the beamwidth and sidelobe performance of the array. Figure 7 shows the experimentally determined beamwidth (BW) and sidelobe (SL) using the new technique on a 36-element linear array compared with (noise-free) simulations of a 63-element multiarm spiral array using conventional beamforming.[27] With conventional beamforming, as seen from Fig. 7, the beamwidth decreases with frequency, implying improved spatial resolution. However, there is a degradation in accuracy, indicated by the SL rejection. The SL rejection for the 63 element multiarm array using conventional beamforming is only 7.5 dB at frequencies greater than 13 kHz.

Note that the source extent, the spatial resolution, and the SL rejection level all contribute to the estimation error. As a general rule, it is impossible to enhance significantly the signal contributions from a particular focal point without also enhancing the contribution from the out-of-focus locations. Recall that we define spatial resolution in terms of localized spatial averages of the source distribution. Thus, an estimate with a spatial resolution of 5 deg at a particular location refers to average intensity in a spatial neighborhood within ±2.5 deg of the focal point. Such a definition of the spatial resolution helps to formulate the constrained optimization problem where one can demand the best spatial resolution for a guaranteed level of accuracy. In particular, as evident in Fig. 7, the new beamforming algorithm achieves a nearly uniform 20 dB or better SL rejection with a 5-deg BW. Conventional approaches provide no such mechanism to trade spatial resolution for accuracy. In summary, the new approach addresses the distributed source localization problem by modifying the beamforming formulation and allows the tradeoff of spatial resolution and accuracy.

Measured noise source distributions obtained from the array for the distributed source at 2 and 10 kHz are shown in Fig. 8. Phased array results are compared with measurements from a near-field sound intensity probe, obtained by using two phase-matched 6.35-mm-diam microphones with a 6-mm spacing. Although they

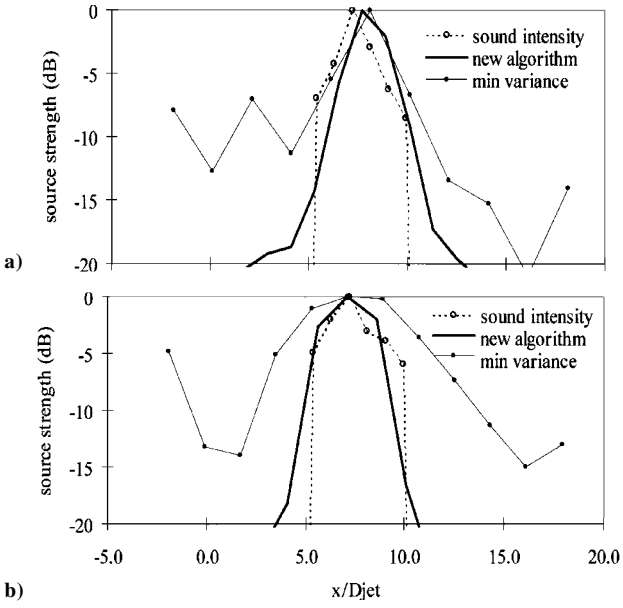

Fig. 8 Source localizations with the new beamformer algorithm compared to minimum variance beamforming and sound intensity measurements at a) 2 kHz and b) 10 kHz.

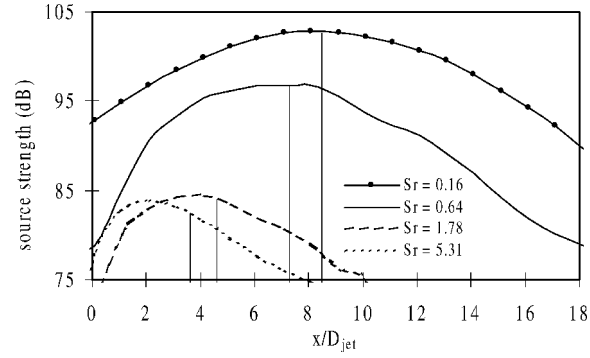

Fig. 9 Noise source distributions for single stream circular jet, M_{jet} = 0.9, and T_{jet} = 538°C.

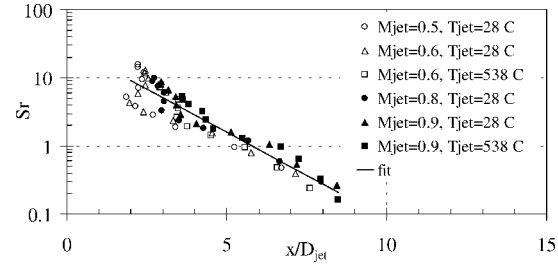

Fig. 10 Noise source distribution centroids for single stream, circular jets over a range of jet Mach numbers and temperatures.

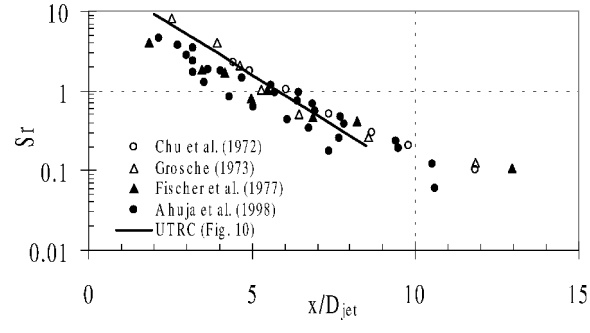

Fig. 11 Present measurement of noise source distribution centroids in circular jets, compared with prior measurements (using other techniques).

contain some approximation errors, sound intensity measurements[28] were considered accurate enough to assess the performance of beamforming algorithms on this distributed source. Figure 8 is a comparison of results from both minimum variance beamforming and those using the new beamforming algorithm. Although both processing techniques located the peak location correctly, the new beamforming result also has significantly reduced SLs, leading to a more accurate estimate of the source amplitude away from the peak location, and spurious sources of much lower amplitude (−20 dB or less). Note that the good agreement shown in Fig. 8 between the new beamforming algorithm and the sound intensity measurements is not a fortuitous result of the array beamwidth, as can be verified by comparison with the smaller beamwidth results shown in Figs. 5 and 7.

III. Jet Noise Source Localization Measurements

The validated technique was applied to the problem of locating noise sources in a high-subsonic, single-stream jet flow issuing into a still ambient inside an anechoic chamber. The noise sources are assumed to be radially compact, but axially noncompact, producing an equivalent noise source distribution on the jet centerline. Flow refraction effects due to gradients within the primary jet (given that no ambient flow was present) were ignored for the array processing because they are expected to introduce relatively small errors in the source location estimate. For the jet noise source measurements reported here, accounting for the spectral averaging errors and those from the array processing, the source amplitudes measured are considered to be accurate to within ±1 dB. The source peak locations (for any given frequency band) are measured reliably to within $1.5D_{jet}$. Parametric studies were performed with the array processing algorithm using a range of spatial resolutions ($0.5–2D_j$) to help converge to a reliable spatial resolution. That is, the spatial resolution parameter was changed until no significant change in the source distributions or amplitudes were noted.

The jet was operated over a range of Mach numbers ($0.5 < M_{jet} < 0.9$) and temperatures ($28 < T_{jet} < 538$°C) to simulate realistic mixed exhaust conditions typically encountered in commercial jet engines. The jet Reynolds numbers (based on D_{jet} and U_{jet}) were in the range 4×10^5–1.5×10^6, with initially turbulent boundary layers. For this study, a 0.083-m-diam round static jet was operated in the ART. The mean flow and temperature fields, the far-field acoustics, and turbulence characteristics associated with the jet have been studied.[10,26] A more detailed analysis of the noise source distributions and their connection with the jet turbulence is reported elsewhere.[10]

Figure 9 shows sample jet noise source distributions measured for $M_{jet} = 0.9$ and $T_{jet} = 538$°C. The high spatial resolution and SL rejection levels provided by the array processing scheme employed here represents a significant improvement over prior source localization methods applied to high-speed jets. At all Strouhal numbers Sr the source distributions have significant spatial extent in the axial direction, although they become more compact and move closer to the nozzle exit at higher Strouhal numbers. The vertical lines associated with each distribution shown in Fig. 9 mark the streamwise centroid positions, to be discussed next.

Figure 10 displays the nondimensional centroid positions of the jet noise source distribution, for different Strouhal numbers and several jet Mach numbers and temperatures. The straight line shown in Fig. 10 is a visual aid to facilitate comparison with published data, shown in Fig. 11. Figure 11 includes data from other source localization techniques applied to unheated round jets: acoustic mirrors[1,2] ($M_{jet} = 1$), polar correlation[6] ($M_{jet} = 0.86$), and two-microphone phase minima[8] ($M_{jet} = 0.89$). In all cases, low-frequency source peaks are located downstream, past the end of the jet potential core (for $x/D_{jet} > 6$), and higher frequency sources are located closer to the jet nozzle exit plane ($x/D_{jet} = 0.0$). No trend in the source

centroid locations is apparent with jet temperature or Mach number. Note, however, differences in the presently measured noise source distributions were observed between the cold and hot jets and are described elsewhere.[10] The new beamforming algorithm presented here offers an alternative approach for accurate jet noise source distribution measurements, avoiding cumbersome repositioning of sensors.

IV. Conclusions

A new beamforming algorithm has been developed that is based on minimizing the ratio of contributions from sources away from the focal region to those from the focal region. The algorithm allows spatial resolution to be traded with accuracy, which ensures uniform performance at different frequencies and with higher confidence amplitude estimates than conventional beamforming approaches. This provides a promising aeroacoustics measurement technique for spatially distributed sources such as those encountered in high-speed jet exhausts.

With conventional beamforming, the decrease of the bandwidth with frequency implies improved spatial resolution but a degradation in accuracy due to higher sidelobes. Thus, it is apparently impossible to enhance signal contributions from a focal point without also enhancing the contribution from out-of-focus locations. In this study, this apparent conflict was resolved by redefining spatial resolution in terms of localized spatial averages of the source distribution. With such a definition, a constrained optimization problem was formulated where the best spatial resolution for a guaranteed level of accuracy can be achieved, permitting a tradeoff between spatial resolution and accuracy. The new algorithm is suited to applications requiring a large dynamic range, high resolution, and high confidence over a broad range of frequencies.

A 36-channel linear phased array was constructed, and the new algorithm was validated with broadband point and distributed sources. The point source experiments demonstrated that with a 5-deg bandwidth the new beamformer achieves a 20-dB sidelobe rejection over the frequency range 1–33 kHz. Also, the new algorithm demonstrated significant improvements over minimum variance beamforming when applied to distributed sources. Finally, the source localization device was applied to explore noise sources over a broad range of frequencies in a high-subsonic, heated jet flow, demonstrating good agreement with prior measurements of noise source centroid positions. Such noise source distribution measurements provide valuable insights into the noise-generation processes and their connection with the turbulent jet flowfield.[10]

Appendix: Accuracy Estimate for New Beamforming Algorithm

The proof for Eq. (13) follows by direct manipulation of the formula for smooth PSD of Eq. (9) and judiciously making use of the properties of Eqs. (10) and (11) of the new beamformer:

$$\bar{\Phi}_s(f,x) = \frac{1}{\delta}\int_{x_0-\delta/2}^{x_0+\delta/2} \Phi_s(f,x)\,\mathrm{d}x$$

$$\approx \frac{1}{\delta}\int_{x_0-\delta/2}^{x_0+\delta/2} |W(f,x_0)H(f,x)|^2\Phi_s(f,x)\,\mathrm{d}x$$

$$= \frac{1}{\delta}\int |W(f,x_0)H(f,x)|^2\Phi_s(f,x)\,\mathrm{d}x$$

$$- \frac{1}{\delta}\int_{x\notin[x_0-\delta/2,x_0+\delta/2]} |W(f,x_0)H(f,x)|^2\Phi_s(f,x)\,\mathrm{d}x$$

$$= \underbrace{\frac{1}{\delta}W(f,x_0)\Phi_y(f)W'(f,x_0)}_{\text{beamformed estimate}} - \frac{\rho}{\delta}\int_\Omega \Phi_s(f,x)w_\delta(x-x_0)\,\mathrm{d}x$$

This implies that the difference between the beamformed estimate and the smooth PSD is given by

$$\left|\bar{\Phi}_s(f,x) - \frac{1}{\delta}W(f,x_0)\Phi_y(f)W'(f,x_0)\right| \le \frac{\rho}{\delta}\int_\Omega \Phi_s(f,x)w_\delta(x-x_0)\,\mathrm{d}x$$

Acknowledgments

Financial support was provided via internal funding at the United Technologies Research Center. The authors thank A. Finn, R. H. Schlinker, and C. Yoerkie for insightful discussions and K. Post and S. Santos for assistance in experiments.

References

[1]Chu, W. T., Laufer, J., and Kao, K., "Noise Source Distribution in Subsonic Jets," *Inter-Noise 72*, Inst. of Noise Control Engineering of the USA, Washington, DC, 1972.

[2]Grosche, F. R., "Distributions of Sound Source Intensities in Subsonic and Supersonic Jets," CP-31, AGARD Paper 4, 1973.

[3]Billingsley, J., and Kinns, R., "The Acoustic Telescope," *Journal of Sound and Vibration*, Vol. 48, No. 4, 1976, pp. 485–510.

[4]Flynn, O. E., and Kinns, R., "Multiplicative Signal Processing for Sound Source Location on Jet Engines," *Journal of Sound and Vibration*, Vol. 46, No. 1, 1976, pp. 137–150.

[5]Laufer, J., Schlinker, R., and Kaplan, R. E., "Experiments on Supersonic Jet Noise," *AIAA Journal*, Vol. 14, No. 4, 1976, pp. 489–497.

[6]Fisher, M. J., Harper-Bourne, M., and Glegg, S. A. L., "Jet Engine Noise Source Locations: the Polar Correlation Technique," *Journal of Sound and Vibration*, Vol. 51, 1977, pp. 23–54.

[7]Fuchs, H. V., "On the Application of Acoustic 'Mirror,' 'Telescope,' and 'Polar Correlation' Techniques to Jet Noise Source Location," *Journal of Sound and Vibration*, Vol. 58, No. 1, 1978, pp. 117–126.

[8]Ahuja, K. K., Massey, K. C., and D'Agostino, M. S., "A Simple Technique of Locating Noise Sources of a Jet Under Simulated Forward Motion," AIAA Paper 98-2359, June 1998.

[9]Bridges, J., "'Measurements' of Jet Acoustic Source Density," AIAA Paper 99-3787, July 1999.

[10]Narayanan, S., Barber, T. J., and Polak, D. R., "High Subsonic Jet Experiments: Turbulence and Noise Generation Studies," *AIAA Journal*, Vol. 40, No. 3, 2002, pp. 430–437.

[11]Freund, J. B., "Noise Sources in a Low-Reynolds-Number Turbulent Jet at Mach 0.9," *Journal of Fluid Mechanics*, Vol. 438, 2001, pp. 277–305.

[12]Johnson, D. H., and Dudgeon, D. E., *Array Signal Processing: Concepts and Techniques*, 1st ed., Signal Processing Series, Prentice–Hall, Upper Saddle River, NJ, 1993.

[13]Piet, J. F., and Elias, G., "Airframe Noise Source Localization Using a Microphone Array," AIAA Paper 97-1643, May 1997.

[14]Hayes, J. A., Horne, W. C., Soderman, P. T., and Brent, P. H., "Airframe Noise Characteristics of a 4.7% Scale DC-10 Model," AIAA Paper 97-1594, May 1997.

[15]Herkes, W. H., and Stoker, R. W., "Wind Tunnel Measurements of the Airframe Noise of a High-Speed Civil Transport," AIAA Paper 98-0472, Jan. 1998.

[16]Michel, U., Barsikow, B., Helbig, J., Hellmig, M., and Schuttpelz, M., "Flyover Noise Measurements on Landing Aircraft with a Microphone Array," AIAA Paper 98-2336, June 1998.

[17]Michel, U., and Qiao, W., "Directivity of Landing Gear Noise Based on Flyover Measurements," AIAA Paper 99-1956, May 1999.

[18]Piet, J. F., Elias, G., and Lebigot, P., "Localization of Acoustic Source from a Landing Aircraft with a Microphone Array," AIAA Paper 99-1811, May 1999.

[19]Barsikow, B., King, W. F., and Pfizenmaier, E., "Wheel/Rail Noise Generated by a High-Speed Train Investigated with a Line Array of Microphones," *Journal of Sound and Vibration*, Vol. 118, No. 1, 1987, pp. 99–122.

[20]Kook, H., Moebs, G. B., Davies, P., and Bolton, J. S., "An Efficient Procedure for Visualizing the Sound Field Radiated by Vehicles During Standardized Passby Tests," *Journal of Sound and Vibration*, Vol. 233, No. 1, 2000, pp. 137–156.

[21]Mammone, R. J., "Inverse Problems and Signal Reconstruction," *Digital Signal Processing Handbook*, edited by V. K. Madisetti and D. B. Williams, CRC Press and IEEE Press, 1997, Sec. 7, pp. 25-1–34-16.

[22]Pillai, U. R., and Burrus, C. S., *Array Signal Processing*, Springer-Verlag, Berlin, 1989.

[23]Humphreys, W. M., Brooks, T. F., Hunter, W. M., and Meadows, K. R., "Design and Use of Microphone Directional Arrays for Aeroacoustic Measurements," AIAA Paper 98-0471, Jan. 1998.

[24]Boyd, S., Ghaoui, L., Feron, E., and Balakrishnan, V., "Linear Matrix Inequalities in System and Control Theory," *Studies in Applied Mathematics*, Vol. 15, Society for Industrial and Applied Mathematics, Philadelphia, 1994.

[25]Paterson, R. W., Vogt, P. G., and Foley, W. M., "Design and Development of the United Aircraft Research Laboratories Acoustic Research Tunnel," *Journal of Aircraft*, Vol. 10, No. 7, 1973, pp. 427–433.

[26]Simonich, J., Narayanan, S., Barber, T. J., and Nishimura, M., "Aeroacoustic Characterization, Noise Reduction, and Dimensional Scaling Effects of High Subsonic Jets," *AIAA Journal*, Vol. 39, No. 11, 2001, pp. 2062–2069.

[27]Underbrink, J. R., and Dougherty, R. P., "Array Design for Non-Intrusive Measurement of Noise Sources," *Noise-Con 96*, Inst. of Noise Control Engineering of the USA, Washington, DC, 1996, pp. 757–762.

[28]Waser, M. P., and Crocker, M. J., "Introduction to the Two-Microphone Cross-Spectral Method of Determining Sound Intensity," *Noise Control Engineering Journal*, Vol. 22, No. 3, 1984, pp. 76–85.

G. M. Faeth
Former Editor-in-Chief